Indentation of thin elastic films glued to rigid substrate: Asymptotic solutions and effects of adhesion

Barış Erbaş[a], Yağmur Ece Aydın[a], Feodor M. Borodich[b]

[a]*Eskişehir Technical University, Department of Mathematics, Yunus Emre Campus, 26470, Eskisehir, Turkey*
[b]*Cardiff University, School of Engineering, Cardiff, CF24 0AA, UK*

Abstract

Indentation of a thin elastic film attached through an interlayer to a rigid support is studied. Because the common interpretations of depth-sensing indentation tests are not applicable to such structured coatings, usually various approximating functions are employed to take into account influence of the interlayer. Contrary to the common approaches, a strict mathematical approach is applied here to study the problems under consideration assuming that the thickness of the two-layer structure is much less than characteristic dimension of the region of contact between the indenter and the coating. A simple derivation of asymptotic relations for displacements and stresses is presented. It is shown that often the leading term approximation to the non-adhesive contact problems is equivalent to contact problem for a Winkler-Fuss elastic foundation with an effective elastic constant. Because the contact between the indenter and the film at nanoscale may be greatly affected by adhesion, the adhesive problem for these bilayer coatings is studied in the framework of the JKR (Johnson, Kendall, and Roberts) theory of adhesion. Assuming the indenter shape near the tip has some deviation from its nominal shape and using the leading term approximation of the layered coatings, the explicit expressions are derived for the values of the pull-off force and for the corresponding critical contact radius of adhesive contact region.

Keywords: thin elastic bilayer, asymptotics, JKR theory, adhesive contact

1. Introduction

Thin solid films having layered structures have enormous areas of applications, in particular in tribological applications. Indeed, recent innovations in coating technology, materials science and surface science has led to the introduction of hard, nanostructured carbon-based coatings, such as amorphous carbon (a-C), diamond-like carbon (DLC), carbon nitride (CN_x), amorphous carbon/tungsten carbide (a-C/WC) nanocomposites, and boron carbide (nominally B_4C), that are often used as solid, low friction lubricating films. However, to use these films as tribological coatings, they must adhere well to the substrate material, otherwise, the high internal stresses would cause film delamination. A comprehensive review of DLC coatings is given by [1]. It was noted that the use of silicon [2] and metallic interlayers such as titanium or chromium [3, 4], may provide good adhesion of carbon-based coatings to many steels.

Another area where layered structures are used is nanoindentation testing of materials. Depth-sensing indentation (DSI) proposed by Kalei [5] is currently a very popular technique for evaluation of mechanical properties of materials of very small volumes. DSI is the continuously monitoring of the $P-\delta$ diagram where P is the applied load and δ is the displacement (the approach of the distant points of the indenter and the sample. DSI can be applied to homogeneous and inhomogeneous solids (see, e.g. [6],[7], [8]), soft and hard thin films [9],[10]) and homogeneous and inhomogeneous thin films (see, e.g. [11],[12]). For example, it has been proposed recently to combine the DSI techniques and transmitted light microscopy, and apply the techniques to very thin and very smooth polished sections (thin films) of the spatially inhomogeneous materials like coals [13]. The material samples prepared as very thin films are often glued to hard substrate. For such very thin films, it is usually possible to apply transmitted light microscopy provided the combination of a material film and a glue layer has thickness of about 10-30μm and the substrate is transparent. The use of thin material samples may vanish the influence of pores and cracks and to visualize the regions of tested components of the inhomogeneous films [14]. However, the application of the traditional methods of interpretation of indentation tests will not allow the researchers to extract the reduced contact modulus of material directly due to the influence of the glue layer and the substrate. In fact, the direct application of the DSI methods could provide only effective (equivalent or composite) elastic modulus of film/glue system. Indeed, the elastic characteristics are estimated usually using methods based on the approach introduced originally by Bulychev et al. [15], that in turn is based on the classic Hertz contact theory, i.e. assuming that contacting solids may be treated as elastic half-spaces, while we study thin solid films connected to the substrate through a thin interlayer or glue. Therefore, the common interpretations of DSI tests are not applicable to structured coatings under investigation. This is the reason that various approximating functions have to be used to estimate the real elastic modulus of the tested component, see [16, 17].

Because the contact problems for layered or coated solids are very important for many practical applications, these problems were studied using various approaches including asymptotic methods. Comprehensive review of approximate and asymptotic approaches to contact problems for an elastic layer may be found in [18, 19, 20]. Formally, the contact problem for an elastic layer may be formulated as an integral equation that was studied mainly by the asymptotic approaches (see, e.g. [19, 21, 22, 23]). However, some of these asymptotic approaches are rather sophisticated even though they are mathematically correct [18, 21]. As Johnson wrote in his famous book (see page 138 in [24]) about the integral equation, the integrand in the formulation has the awkward form and this has led to serious difficulties in the analysis of contact stresses in strips and layers. On the other hand, there are two effective asymptotic methods that can be employed for studying the problems under consideration without employment of the integral formulation: (i) the Argatov-Mishuris (AM) method [19] and (ii) Goldenveizer-Kaplunov-Nolde (GKN) one [25, 26].

The GKN method is based on direct asymptotic integration of the main equation. The method was originally developed for applications in theory of plates and shells [25, 26]. Later, it was shown that the GKN method may be applied to two-dimensional contact problems [27] and to three-dimensional contact problem for a single elastic layer [20]. It has been recently shown within the AM approach that the contact problem for a thin isotropic or transversely isotropic layer in leading order asymptotic approximation is reduced to the problem for a Winkler-Fuss layer (see page 14 in [19], also [28]). The same result was obtained for a single elastic layer using the GKN approach [20] and here these results are developed further in application to the problem of indentation of a bi-layer coating (an elastic layer glued to a rigid substrate). The term 'glue' is used here for any material layer that connects the thin solid coating and a rigid substrate, in particular it may be silicon, chromium or epoxy polymer layer. The interlayer (the glue layer) is also modelled as an elastic thin film. Using the GKN method, a clear asymptotic solution to the problem is derived in the case when the size of contact region is much greater than the thickness of the elastic compressible film. It has been shown that indentation of the two-layer system under investigation in leading order of the asymptotic approximation may represent the Winkler-Fuss elastic foundation with an effective elastic spring constant. This allows us to obtain the expressions for displacements and stresses acting in both the elastic film and the glue layer.

Because the DSI techniques are especially important when mechanical properties of materials are studied using very small volumes of materials such as thin films, the present asymptotic approach may be used in material testing. Usually problems of DSi are studied without taking into account adhesive interactions. However, as it was noted by Kendall, the nano-world is the Sticky Universe [29]. Thus, to study nanoindentation, the adhesive interactions should be taken into account. The adhesive indentation is studied in the framework of a modified JKR (Johnson, Kendall and Roberts) theory [30]. It has been shown that the current approach to the problem of adhesive indentation is equivalent mathematically to the approach presented in [20].

It is usually assumed that the indenter is a sharp pyramid or a cone. However, the indenter shape near the tip has some deviation from its nominal shape. The shapes of these non-ideal shaped indenters may be well approximated as monomial functions of radius

$$f(r) = B_d r^d, \quad d \geq 1 \tag{1}$$

where B_d is the constant of the shape of the monomial function of degree d (see, [31, 32, 33] for details). For indenters having deviation from their nominal shapes, we examine the case of power-law shaped probes (1) in detail. We also present some illustrative examples of adhesive indentation into a diamond-like carbon film and into a ultra-thin ceramic film. The obtained results are compared with non-adhesive solutions.

2. Formulation of non-adhesive contact problem

The classic formulation of the Hertz-type contact problems (see references in [34]) assumes that the shape of the bodies and the compressing force P are given and molecular adhesion can be ignored. Hence, the fields of displacements and stresses appear in the solids only after the external load is applied. In addition, it is assumed that the contact region is small in comparison with the main radii of curvature of contacting solids and, therefore the boundary value problem for contacting solids may be formulated as a boundary value problem for an isotropic elastic half-space. Because we do not consider here a contact problem for an elastic half-space but rather action of a smooth, convex rigid indenter on an elastic bilayered coatings, the classic theory is not applicable.

Let us use both the Cartesian and cylindrical coordinate frames, namely $x_1 = x, x_2 = y, x_3 = z$ and r, θ, z, where $r = \sqrt{x^2 + y^2}$ and $x = r\cos\theta, y = r\sin\theta$. Let us place the origin (O) of Cartesian coordinates at the point of initial contact between the indenter and the layer. Let us direct the axis of x_3 along the normal to the layer towards the inside of the layer (see Fig. 1).

Let us consider a rigid indenter whose surface is described by a function f, i.e., $x_3 = -f(x_1, x_2)$, $f \geqslant 0$. This indenter is pressed by the force P to a boundary of the contacting solid. After the indenter contacts with the layer, the displacements u_i and stresses σ_{ij} are generated.

Equations of equilibrium may then be written as

$$(\sigma_\alpha)_{i1,1} + (\sigma_\alpha)_{i2,2} + (\sigma_\alpha)_{i3,3} = 0, \qquad \alpha = l, g. \tag{2}$$

Here and henceforth α is a categorical variable that can take on one of the two following values: l and g that denote the thin layer (the film) and the glue (the interlayer), respectively.

The constitutive relations for the linear elastic materials are represented by

$$(\sigma_\alpha)_{ij} = \lambda_\alpha\, \delta_{ij}(u_\alpha)_{k,k} + \mu_\alpha\left((u_\alpha)_{i,j} + (u_\alpha)_{j,i}\right), \tag{3}$$

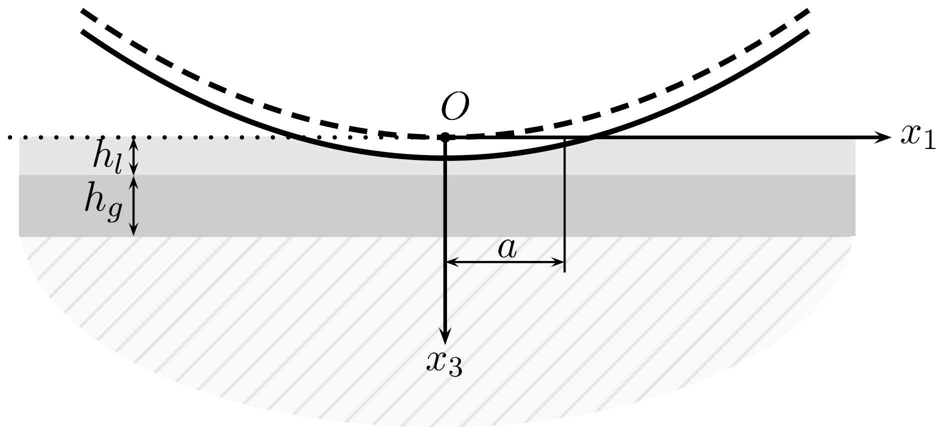

Figure 1: Problem formulation for a thin elastic film attached through an interlayer to a rigid support. O is the coordinate origin; h_l and h_g are the thickness of the layer and interlayer (glue) respectively; a is the contact radius. The dashed line is the indenter profile at the beginning of indentation.

where $(u_\alpha)_i$ are components of the displacement vector, δ_{ij} is the Kronecker delta, and E_α, ν_α, are the elastic modulus and the Poisson's ratio respectively, and λ_α, and μ_α are the Lamé constants

$$\lambda_\alpha = \frac{E_\alpha \nu_\alpha}{(1+\nu_\alpha)(1-2\nu_\alpha)}, \qquad \mu_\alpha = \frac{E_\alpha}{2(1+\nu_\alpha)}. \tag{4}$$

The boundary conditions should describe the problem out of the contact region G, within the region and conditions describing interactions between the layer and the support. Because the problem is frictionless, we have

$$(\sigma_l)_{3j}(x_1, x_2, 0) = 0, \quad (x_1, x_2) \in \mathbb{R}^2 \quad j = 1, 2. \tag{5}$$

The contact region G is defined as an open region such that if $(x_1, x_2) \in G$ then the gap $(u_3 - g)$ between the punch and the half-space is equal to zero and surface stresses are non-positive, while outside the contact region, i.e. for $(x_1, x_2) \in \mathbb{R}^2 \setminus G$, the gap is positive and the stresses are equal to zero. Hence, the additional to (5) boundary conditions within the contact region G describe the action of an indenter on the layer can be written as

$$\begin{array}{ll} (u_l)_3(x_1, x_2, 0) = g(x_1, x_2), & x_3 = 0, \quad (x_1, x_2) \in G, \\ (\sigma_l)_{3j} = 0, & x_3 = 0, \quad (x_1, x_2) \in \mathbb{R}^2 \setminus G \end{array} \tag{6}$$

The continuity of stresses and displacements along the interface are given by

$$(\sigma_l)_{i3} = (\sigma_g)_{i3} \quad \text{and} \quad (u_l)_i = (u_g)_i, \quad i = 1, 2, 3, \quad \text{for} \quad x_3 = h_l. \tag{7}$$

Because the glue is bounded to the support, one can write the interaction between the glue and the rigid support as

$$(u_g)_i = 0, \quad i = 1, 2, 3, \quad \text{for} \quad x_3 = h_l + h_g. \tag{8}$$

For the general case of the problem of vertical frictionless pressing, we have

$$g(\mathbf{x}) = \delta - f(x_1, x_2) = \delta - \varphi\left(\frac{x_1}{a}, \frac{x_2}{a}\right), \quad f(x_1, x_2) \equiv \varphi\left(\frac{x_1}{a}, \frac{x_2}{a}\right). \tag{9}$$

In addition, there is the integral condition

$$\int_{\mathbb{R}^2} (\sigma_l)_{33}(x_1, x_2, 0) dx_1 dx_2 = -P. \tag{10}$$

3. The GKN asymptotic approaches to contact problem for an elastic layers

According to the ideas of the GKN asymptotic integration procedure, first we dilate the scale of the independent variables for both layers and assume that differentiation with respect to the scaled variables does not change the asymptotic order of the quantities to be found. Thus, we introduce the following dimensionless variables

$$\xi_1 = \frac{x_1}{a}, \qquad \xi_2 = \frac{x_2}{a}, \qquad \xi_3 = \frac{x_3}{h_l}. \tag{11}$$

We assume also that the thickness of the film is small compared to the radius of contact, i.e. the parameter

$$\varepsilon = h_l/a \tag{12}$$

is small. Following the GKN asymptotic procedure, the displacement and stress components may be expressed through the asymptotic orders

$$\begin{aligned}
&(u_\alpha)_j\,(x_1,x_2,x_3) = h_l\varepsilon(u^*_\alpha)_j\,(\xi_1,\xi_2,\xi_3)\,, \qquad j=1,2,\\
&(u_\alpha)_3\,(x_1,x_2,x_3) = h_l(u^*_\alpha)_3\,(\xi_1,\xi_2,\xi_3)\,,\\
&(\sigma_\alpha)_{ii}\,(x_1,x_2,x_3) = \mu_l\,(\sigma^*_\alpha)_{ii}\,(\xi_1,\xi_2,\xi_3)\,,\\
&(\sigma_\alpha)_{j3}\,(x_1,x_2,x_3) = (\sigma_\alpha)_{3j}\,(\xi_1,\xi_2,\xi_3) = \mu_l\,\varepsilon(\sigma^*_\alpha)_{j3}\,(\xi_1,\xi_2,\xi_3)\,,\\
&(\sigma_\alpha)_{12}\,(x_1,x_2,x_3) = (\sigma_\alpha)_{21}\,(\xi_1,\xi_2,\xi_3) = \mu_l\,\varepsilon^2(\sigma^*_\alpha)_{12}\,(\xi_1,\xi_2,\xi_3)\,,
\end{aligned} \tag{13}$$

where quantities with asterisks are assumed to be dimensionless functions of the same asymptotic order.

Substituting (11) into (13), the governing equations may be rewritten in the dimensionless quantities as

$$\begin{aligned}
&(\sigma^*_\alpha)_{11,1} + \varepsilon^2(\sigma^*_\alpha)_{12,2} + (\sigma^*_\alpha)_{13,3} = 0,\\
&\varepsilon^2(\sigma^*_\alpha)_{12,1} + (\sigma^*_\alpha)_{22,2} + (\sigma^*_\alpha)_{23,3} = 0,\\
&\varepsilon^2\left((\sigma^*_\alpha)_{13,1} + (\sigma^*_\alpha)_{23,2}\right) + (\sigma^*_\alpha)_{33,3} = 0,\\
&(\sigma^*_\alpha)_{11} = (\mu_\alpha/\mu_l)\left(\varepsilon^2\left(k^2_\alpha(u^*_\alpha)_{1,1} + (k^2_\alpha-2)\,(u^*_\alpha)_{2,2}\right) + (k^2_\alpha-2)\,(u^*_\alpha)_{3,3}\right),\\
&(\sigma^*_\alpha)_{22} = (\mu_\alpha/\mu_l)\left(\varepsilon^2\left((k^2_\alpha-2)\,(u^*_\alpha)_{1,1} + k^2_\alpha(u^*_\alpha)_{2,2}\right) + (k^2_\alpha-2)\,(u^*_\alpha)_{3,3}\right),\\
&(\sigma^*_\alpha)_{33} = (\mu_\alpha/\mu_l)\left(\varepsilon^2\,(k^2_\alpha-2)\left((u^*_\alpha)_{1,1} + (u^*_\alpha)_{2,2}\right) + k^2_\alpha(u^*_\alpha)_{3,3}\right),\\
&(\sigma^*_\alpha)_{12} = (\mu_\alpha/\mu_l)\left((u^*_\alpha)_{1,2} + (u^*_\alpha)_{2,1}\right), \qquad (\sigma^*_\alpha)_{13} = (\mu_\alpha/\mu_l)\left((u^*_\alpha)_{1,3} + (u^*_\alpha)_{3,1}\right),\\
&(\sigma^*_\alpha)_{23} = (\mu_\alpha/\mu_l)\left((u^*_\alpha)_{2,3} + (u^*_\alpha)_{3,2}\right),
\end{aligned} \tag{14}$$

with comma in the subscript denoting differentiation with respect to the corresponding dimensionless variable ξ_j and

$$k^2_\alpha = \frac{2-2\nu_\alpha}{1-2\nu_\alpha}. \tag{15}$$

We consider only compressible materials, i.e. $\nu_\alpha \neq 0.5$ and therefore, $1-2\nu_\alpha \neq 0$.

The boundary conditions (6) and (8) can respectively be represented as

$$\begin{aligned}
(u^*_l)_3\,(\xi_1,\xi_2,0) =& \frac{1}{h_l}\left(\delta - \varphi\,(\xi_1,\xi_2)\right), \qquad (\xi_1,\xi_2)\in G^*,\\
(\sigma^*_l)_{13}\,(\xi_1,\xi_2,0) =& (\sigma^*_l)_{23}\,(\xi_1,\xi_2,0) = 0,
\end{aligned} \tag{16}$$

while (8) is transformed to the following

$$(u^*_g)_1\,(\xi_1,\xi_2,1+h_r) = (u^*_g)_2\,(\xi_1,\xi_2,1+h_r) = (u^*_g)_3\,(\xi_1,\xi_2,1+h_r) = 0$$

where G^* is the region of contact in the (ξ_1, ξ_2)-plane and h_r defined as the ratio of the interlayer (glue) and the thin film thicknesses, i.e., $h_r = h_g/h_l$. The continuity conditions (7), in this case, become

$$\mu_l(\sigma_l^*)_{i3} = \mu_g(\sigma_g^*)_{i3} \quad \text{and} \quad (u_l^*)_i = (u_g^*)_i, \quad \text{for} \quad \xi_3 = 1. \tag{17}$$

To reduce the number of unknowns, we transform (14) into the form of Lamé equations, keeping only unknown displacements

$$\begin{aligned} \left(k_\alpha^2 - 1\right)(u_\alpha^*)_{3,13} + (u_\alpha^*)_{1,33} + \varepsilon^2\left(k_\alpha^2(u_\alpha^*)_{1,11} + (u_\alpha^*)_{1,22} + \left(k_\alpha^2 - 1\right)(u_\alpha^*)_{2,12}\right) = 0 \\ \left(k_\alpha^2 - 1\right)(u_\alpha^*)_{3,23} + (u_\alpha^*)_{2,33} + \varepsilon^2\left((u_\alpha^*)_{2,11} + k_\alpha^2(u_\alpha^*)_{2,22} + \left(k_\alpha^2 - 1\right)(u_\alpha^*)_{1,12}\right) = 0 \\ k_\alpha^2(u_\alpha^*)_{3,33} + \varepsilon^2\left((u_\alpha^*)_{3,11} + (u_\alpha^*)_{3,22} + \left(k_\alpha^2 - 1\right)((u_\alpha^*)_{1,13} + (u_\alpha^*)_{2,23})\right) = 0. \end{aligned} \tag{18}$$

Equations (18) contain only terms of order ε^2, therefore the following asymptotic expansion may be employed

$$(u_\alpha^*)_i = (u_\alpha^0)_i + \varepsilon^2(u_\alpha^1)_i + \varepsilon^4(u_\alpha^2)_i + \ldots \qquad i = 1, 2, 3 \tag{19}$$

Note that $(u_\alpha^k)_i$ are *dimensionless* asymptotic approximations of k-th order for i-th component of displacement within both the material layer ($\alpha = l$) and the glue ($\alpha = g$).

Thus, the leading order approximation to the non-adhesive contact problems is reduced to the following boundary value problems for the inner (the film of the tested material, i.e. $\alpha = l$) and outer (the glue, i.e. $\alpha = g$) layers, respectively,

$$\left(k_\alpha^2 - 1\right)(u_\alpha^0)_{3,13} + (u_\alpha^0)_{1,33} = 0, \quad \left(k_\alpha^2 - 1\right)(u_\alpha^0)_{3,23} + (u_\alpha^0)_{2,33} = 0, \quad k_\alpha^2(u_\alpha^0)_{3,33} = 0.$$

In this case, the boundary conditions at $\xi_3 = 0$ become

$$(u_l^0)_3 = \frac{1}{h_l}\left(\delta - \varphi\left(\xi_1, \xi_2\right)\right), \qquad (u_1^0)_{1,3} + (u_l^0)_{3,1} = 0, \qquad (u_l^0)_{2,3} + (u_l^0)_{3,2} = 0,$$

together with the continuity of the displacements and stresses at the interface of the film and the interlayer, i.e. at $\xi_3 = 1$ given by

$$\begin{aligned} (u_l^0)_i = (u_g^0)_i, \quad \mu_l((u_l^0)_{1,3} + (u_l^0)_{3,1}) = \mu_g((u_2^0)_{1,3} + (u_2^0)_{3,1}), \\ \mu_l((u_l^0)_{2,3} + (u_l^0)_{3,2}) = \mu_g((u_2^0)_{2,3} + (u_2^0)_{3,2}), \quad \mu_l k_l^2(u_l^0)_{3,3} = \mu_g k_g^2(u_g^0)_{3,3}, \end{aligned} \tag{20}$$

and, becuse the interlayer is firmly connected to the rigid substrate, we have also the conditions

$$(u_g^0)_1 = (u_g^0)_2 = (u_g^0)_3 = 0, \qquad \xi_3 = 1 + h_r. \tag{21}$$

Further, we consider only the above leading-order approximation of the problem.

3.1. Solution for displacements for the leading-order problem

From the third equation in (20), it follows that

$$(u_l^0)_3 = \xi_3 F_l\left(\xi_1, \xi_2\right) + F_g\left(\xi_1, \xi_2\right), \qquad (u_g^0)_3 = \xi_3 G_l\left(\xi_1, \xi_2\right) + G_g\left(\xi_1, \xi_2\right), \tag{22}$$

while from the first and last equations in (20) and the boundary conditions, it follows that $F_g = (\delta - \varphi)/h_r$ and $G_g = -(1 + h_r)G_l$.

Next, by using the continuity condition for the third component of displacement and σ_{33} from the equation (20), we obtain

$$F_l = -\frac{1}{h_l(1+h_r\mu_r\kappa_r^2)}(\delta-\varphi), \qquad G_l = \mu_r\kappa_r^2 F_l \tag{23}$$

where the dimensionless quantities μ_r and κ_r are defined as the following ratios

$$\mu_r = \frac{\mu_l}{\mu_g}, \qquad \kappa_r = \frac{k_l}{k_g}. \tag{24}$$

Then it follows from (22) - (24)

$$(u_l^0)_3\,(\xi_1,\xi_2,\xi_3) = \frac{1}{h_l}\left(\delta-\varphi\left(\xi_1,\xi_2\right)\right)\left(1-\frac{\xi_3}{(1+h_r\mu_r\kappa_r^2)}\right), \tag{25}$$

$$(u_g^0)_3\,(\xi_1,\xi_2,\xi_3) = -\left(\xi_3-(1+h_r)\right)\left(\delta-\varphi\left(\xi_1,\xi_2\right)\right)\frac{\mu_r\kappa_r^2}{h_l(1+h_r\mu_r\kappa_r^2)}. \tag{26}$$

Below, we present the derivation of the normal stresses, tangential displacements and, also, the shear stresses omitting the details of the derivation.

3.2. Normal stresses in the thin layer

Considering just the leading term of the asymptotic approximation of the displacements, i.e. $(u_\alpha^*)_i \approx (u_\alpha^0)_i$, $i=1,2,3$, we obtain from (14) that

$$\begin{aligned}
(\sigma_\alpha^*)_{11} &\approx \frac{\mu_\alpha}{\mu_l}\left(k_\alpha^2-2\right)(u_\alpha^*)_{3,3}, & (\sigma_\alpha^*)_{12} &= \frac{\mu_\alpha}{\mu_l}\left((u_\alpha^*)_{1,2}+(u_\alpha^*)_{2,1}\right),\\
(\sigma_\alpha^*)_{22} &\approx \frac{\mu_\alpha}{\mu_l}\left(k_\alpha^2-2\right)(u_\alpha^*)_{3,3}, & (\sigma_\alpha^*)_{13} &= \frac{\mu_\alpha}{\mu_l}\left((u_\alpha^*)_{1,3}+(u_\alpha^*)_{3,1}\right),\\
(\sigma_\alpha^*)_{33} &\approx \frac{\mu_\alpha}{\mu_l}k_\alpha^2(u_\alpha^*)_{3,3}, & (\sigma_\alpha^*)_{23} &= \frac{\mu_\alpha}{\mu_l}\left((u_\alpha^*)_{2,3}+(u_\alpha^*)_{3,2}\right).
\end{aligned}$$

Therefore, the normalized stresses of the leading order approximation are

$$\begin{aligned}
(\sigma_\alpha^*)_{ii} &\approx -(k_\alpha^2-2)\frac{k_\beta^2}{h_\alpha(k_\beta^2+h_r k_\alpha^2)}\left(\delta-\varphi\right), \qquad \alpha\neq\beta, \quad \alpha,\beta=l,g, \quad i=1,2.\\
(\sigma_\alpha^*)_{33} &\approx -\frac{k_l^2}{h_l(1+h_r\kappa_r^2)}\left(\delta-\varphi\right).
\end{aligned} \tag{27}$$

Let us write the above solution for the leading order approximation in dimensional variables. Using the scaling expressions (13), we obtain for the displacements

$$(u_l)_3 = h_l(u_l^*)_3 \approx \left(\delta-\varphi\left(\xi_1,\xi_2\right)\right)\left(1-\frac{\xi_3}{(1+h_r\mu_r\kappa_r^2)}\right), \tag{28}$$

$$(u_g)_3 = h_l(u_g^*)_3 \approx -h_l(\xi_3-(1+h_r))\left(\delta-\varphi\left(\xi_1,\xi_2\right)\right)\frac{\kappa^2}{h_l(1+h_r\mu_r\kappa_r^2)}. \tag{29}$$

It is not difficult to see that the leading order normal stress $(\sigma_l^*)_{33}$ may be presented, on using the third equation of (13) and (27), in the dimensional form

$$(\sigma_l)_{33} \approx -\frac{\mu_l k_l^2}{h_l(1+h_r\mu_r\kappa_r^2)}\left(\delta-\varphi\right) = -\left(\frac{h_l}{\mu_l k_l^2}+\frac{h_g}{\mu_g k_g^2}\right)^{-1}\left(\delta-\varphi\right)$$

and inserting k_α and μ_α in terms of ν_α and E_α into the latter equation we arrive at, employing (4) and (15),

$$(\sigma_l)_{33} \approx \left(\frac{h_l(1+\nu_l)(1-2\nu_l)}{E_l(1-\nu_l)} + \frac{h_g(1+\nu_g)(1-2\nu_g)}{E_g(1-\nu_g)}\right)^{-1}(\delta-\varphi).$$

The coefficient of the last equation may be rewritten in the form

$$K_\Sigma = \left(\frac{1}{K_l} + \frac{1}{K_g}\right)^{-1} \quad \text{with} \quad K_\alpha = \frac{E_\alpha(1-\nu_\alpha)}{h_\alpha(1+\nu_\alpha)(1-2\nu_\alpha)}. \tag{30}$$

It is not difficult to recognize that the physical dimension of this coefficient equals to that of K_l or K_g, namely FL^{-3}. It is also worth mentioning that the physical dimension of the coefficient in question differs from that of the spring constant of Hooke's law which is FL^{-1}.

It follows from (13) and (27), that the leading term approximation to the non-adhesive contact problems for a thin elastic layer connected through an elastic interlayer to a rigid substrate is equivalent to contact problem for a Winkler-Fuss elastic foundation with an effective elastic constant K_Σ

$$(\sigma_l)_{33} \approx -K_\Sigma\,(\delta-\varphi) \tag{31}$$

where K_Σ is the effective elastic spring constant of the foundation (the effective foundation modulus). The contact pressure $p = -\left.(\sigma_l)_{33}\right|_{\xi_3=0}$ in the leading-order approximation is

$$p = K_\Sigma\,(\delta-\varphi)\,. \tag{32}$$

3.3. Tangential displacements and shear stresses in the thin layer

We have derived above the expressions for the vertical components of displacements ($\boldsymbol{u}_l$) and ($\boldsymbol{u}_g$) together with normal components of stresses ($\boldsymbol{\sigma}_l$) and ($\boldsymbol{\sigma}_g$) for the thin film and the interlayer, respectively. Now we present the expressions of the tangential displacements together with the shear stresses omitting the details of derivations. We remind that the subindex r has the same meaning as above, i.e. r means that the variable is a ratio of two variables having the same physical dimension.

Equations for $(u_l^0)_j$ and $(u_g^0)_j$, $j=1,2$, are given by

$$\begin{aligned}(u_l^0)_j =& \frac{1}{2h_l(1+h_r\mu_r\kappa_r^2)}\left[-\xi_3^2(k_l^2-1)+2(\xi_3-1)(1+h_r\mu_r\kappa_r^2)+(k_l^2-1)-\mu_r\kappa_r^2(k_g^2-1)\left(1-(1+h_r)^2\right)\right.\\ &\left.-2h_r\mu_r\left((2-k_l^2)-\kappa_r^2(1-k_g^2-h_r)\right)\right]\varphi_{,j}, \qquad (33)\\ (u_g^0)_j =& \frac{\mu_r}{2h_l(1+h_r\mu_r\kappa_r^2)}\left[((1+h_r)^2-\xi_3^2)(k_g^2-1)\kappa_r^2+2(\xi_3-(1+h_r))(2-k_l^2-\kappa_r^2(1-h_r-k_g^2))\right]\varphi_{,j}.\end{aligned}$$

The normalized tangential stresses of the leading order approximation for the thin film are

$$\begin{aligned}(\sigma_l^*)_{12} \approx& -\frac{1}{h_l(1+h_r\mu_r\kappa_r^2)}\left[-\xi_3^2(k_l^2-1)+2\xi_3(1+h_r\mu_r\kappa_r^2)+(k_l^2-1)-\mu_r\kappa_r^2(k_g^2-1)\left(1-(1+h_r)^2\right)\right.\\ &\left.-2h_r\mu_r\left((2-k_l^2)-\kappa_r^2(1-k_g^2-h_r)\right)\right]\varphi_{,12}, \qquad (34)\\ (\sigma_l^*)_{j3} \approx& \,\xi_3\frac{(2-k_l^2)}{h_l(1+h_r\mu_r\kappa_r^2)}\varphi_{,j}.\end{aligned}$$

whereas for the interlayer, they are given by

$$\begin{aligned}(\sigma_g^*)_{12} \approx& \frac{1}{\mu_r h_l(1+h_r\mu_r\kappa_r^2)}\left[((1+h_r)^2-\xi_3^2)(k_g^2-1)\kappa_r^2+2(\xi_3-(1+h_r))(2-k_l^2-\kappa_r^2(1-h_r-k_g^2))\right]\varphi_{,21},\\ (\sigma_g^*)_{j3} \approx& \frac{1}{h_l(1+h_r\mu_r\kappa_r^2)}\left[(1-\xi_3)(k_g^2-2)\kappa_r^2+2-k_l^2\right]\varphi_{,j}. \qquad (35)\end{aligned}$$

Using (13), we may write displacement components for the thin elastic film as

$$(u_l)_j = \varepsilon h_l (u_l^*)_j \approx \frac{h_l}{2a(1+h_r\mu_r\kappa_r^2)}\left[-\xi_3^2(k_l^2-1)+2(\xi_3-1)(1+h_r\mu_r\kappa_r^2)+(k_l^2-1)-\right.$$
$$\left.\mu_r\kappa_r^2(k_g^2-1)\left(1-(1+h_r)^2\right)-2h_r\mu_r\left((2-k_l^2)-\kappa_r^2(1-k_g^2-h_r)\right)\right]\varphi_{,j}, \qquad (36)$$

and, finally, for the inter layer, the corresponding displacements take the form

$$(u_g)_j = \varepsilon h_l (u_g^*)_j \approx \frac{\mu_r h_l}{2a(1+h_r\mu_r\kappa_r^2)}\left[((1+h_r)^2-\xi_3^2)(k_g^2-1)\kappa_r^2+2(\xi_3-(1+h_r))\times\right.$$
$$\left.(2-k_l^2-\kappa_r^2(1-h_r-k_g^2))\right]\varphi_{,j}. \qquad (37)$$

4. Adhesive contact problems for a glued coating

Mechanics of adhesive contact is an active field of research (see, e.g. a review in [34]). Here we study the problem of adhesive indentation into a glued coating within the framework of the JKR theory. Originally the theory was developed for contact of isotropic elastic spheres [35, 29]. The theory was based on the combination of the Derjaguin idea of calculation of the total energy of adhesive contact, the so-called Derjaguin approximation [36], and the brilliant idea of splitting the calculations of the energy into two simple steps: the energy of non-adhesive contact between two elastc spheres and the contact energy for a flat ended cylinder [35]. Borodich noted that if one derives an expression for the slope of the force-displacement curve of an appropriate problem of non-adhesive contact then the JKR theory may be extended to the problem of adhesive contact for an axisymmetric convex indenter of arbitrary profile. These problems were solved for transversely isotropic elastic materials [37], prestressed materials [34], a two-dimensional stretched membrane [38], isotropic frictional indenter [33], and a single thin isotropic layer [20]. Here, we extend the above ideas to problem of adhesive indentation into a bilayer elastic coating.

If an axisymmetric convex, smooth indenter of arbitrary profile is in contact a simple Winkler-Fuss elastic foundation whose elastic properties are characterized by the foundation modulus K_Σ then the slope of the $\delta - P$ curve at any point is

$$S = \frac{dP}{d\delta} = \pi a^2 K_\Sigma. \qquad (38)$$

Using (38) it is possible to show that for an arbitrary convex body of revolution $f(r)$, $f(0) = 0$, the JKR theory leads to the following expressions

$$P = P_{NA}(a) - \sqrt{2wK_\Sigma}\pi a^2, \quad \delta = \delta_{NA} - \sqrt{\frac{2w}{K_\Sigma}}. \qquad (39)$$

The latter of the above expressions can be written as

$$\delta = f(a) - \left(\frac{2w}{K_\Sigma}\right)^{1/2}. \qquad (40)$$

Here, $P_{NA}(a)$ is the load that correspond to the contact radius a in a non-adhesive contact between the glued coating and the indenter, $\delta_{NA}(a)$ is the displacement of the indenter that has the contact region of radius a in the non-adhesive contact problem, w is the specific work of adhesion of the contacted materials.

For indenters, whose shape is described by (1), the general expressions (39) and (40) have the following form

$$P = \pi K_\Sigma \left(\frac{d}{d+2} B_d a^{d+2} - \sqrt{\frac{2w}{K_\Sigma}} a^2 \right) \tag{41}$$

and

$$\delta = B_d a^d - \sqrt{\frac{2w}{K_\Sigma}}. \tag{42}$$

It follows from (41) that at $P = 0$ the radius a of the contact region and the corresponding shift of the origin of the displacement axis $\delta_s = \delta[a(0)]$ are

$$a(0) = \left(\frac{d+2}{dB_d} \sqrt{\frac{2w}{K_\Sigma}} \right)^{1/d}, \qquad \delta_s = \delta[a(0)] = \frac{2}{d} \sqrt{\frac{2w}{K_\Sigma}}. \tag{43}$$

The maximum absolute value of the adherence force $P_c = -P(a_c)$ is achieved at

$$a_c = \left(\frac{2}{dB_d} \sqrt{\frac{2w}{K_\Sigma}} \right)^{1/d}. \tag{44}$$

Substituting (44) into (41), we obtain

$$P_c = -P(a_c) = \pi K_\Sigma \frac{d}{d+2} \left(\frac{2}{dB_d} \right)^{2/d} \left(\frac{2w}{K_\Sigma} \right)^{(2+d)/2d}. \tag{45}$$

Let us take $a(0)$ as the characteristic parameter. Then the characteristic parameters of the adhesive contact problems that can be used to write dimensionless variables of adhesive contact problem can be chosen as

$$a^* = a(0), \quad P^* = \pi K_\Sigma \left(\frac{d+2}{dB_d} \right)^{\frac{2}{d}} \left(\frac{2w}{K_\Sigma} \right)^{\frac{2+d}{2d}}, \quad \delta^* = \sqrt{\frac{2w}{K_\Sigma}}. \tag{46}$$

Then (41) and (42) have the following dimensionless form

$$P/P^* = (a/a^*)^{d+2} - (a/a^*)^2 \tag{47}$$

and

$$\frac{\delta}{\delta^*} = \frac{d+2}{d} \left(\frac{a}{a^*} \right)^d - 1. \tag{48}$$

The graph of dimensionless dependency (47) for several values of degree d is represented on Fig. 2

It follows from (41) and (42) that the relation $P(\delta)$ can be expressed not only in a parametric form but also as an explicit relation

$$P = \frac{\pi K_\Sigma}{d+2} \left[\frac{1}{B_d} \left(\delta + \sqrt{\frac{2w}{K_\Sigma}} \right) \right]^{2/d} \left(\delta d - 2\sqrt{\frac{2w}{K_\Sigma}} \right). \tag{49}$$

or in the dimensionless form

$$\frac{P}{P^*} = \left[\frac{d}{d+2} \left(\frac{\delta}{\delta^*} + 1 \right) \right]^{(d+2)/d} - \left[\frac{d}{d+2} \left(\frac{\delta}{\delta^*} + 1 \right) \right]^{2/d}. \tag{50}$$

The graphs of the dimensionless explicit relation (50) is represented on Fig. 3

The graphs above can be used to obtain the 0-th asymptotic approximation of the problem of adhesive contact between an axisymmetric indenter and a thin isotropic or transversely isotropic elastic layer.

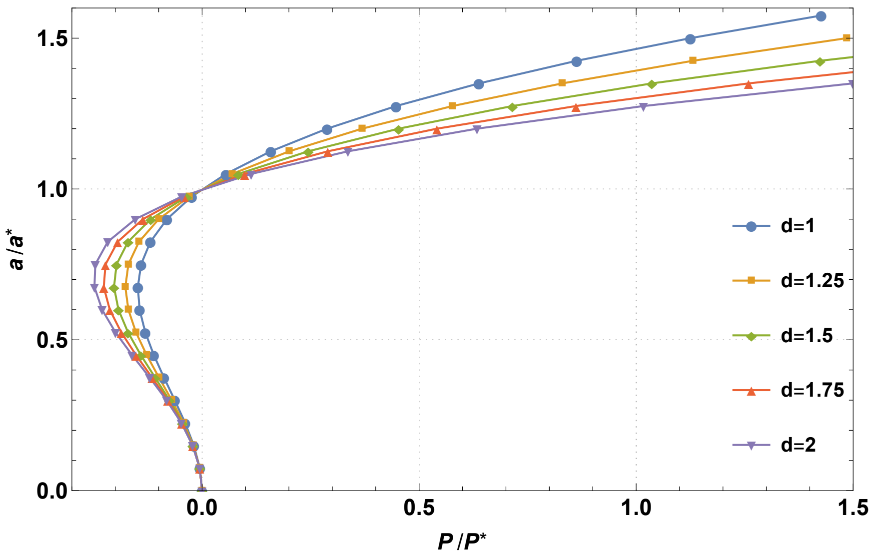

Figure 2: The dimensionless graphs of the force-radius curves (47) for blunt indenters when the power-law exponent d varies from $d = 1$ (cone) to $d = 2$ (sphere).

5. Particular cases of indenters and examples

We will consider, here, the cases of spherical and conical indenters along with some examples of specific materials.

5.1. Spherical indenters

For a spherical indenter of radius R, we can represent the indenter shape as a paraboloid of revolution ($d = 2$ and $B_2 = (2R)^{-1}$), then it follows from (41) and (42) that

$$\begin{aligned} P &= \pi K_\Sigma \left(\frac{1}{4R} a^4 - \sqrt{\frac{2w}{K_\Sigma}} a^2 \right) \\ \delta &= a^2/(2R) - \sqrt{\frac{2w}{K_\Sigma}}. \end{aligned} \tag{51}$$

and from (49) the explicit force-displacement relation follows as

$$P = \pi K_\Sigma R \left[\left(\delta + \sqrt{\frac{2w}{K_\Sigma}} \right) \left(\delta - \sqrt{\frac{2w}{K_\Sigma}} \right) \right] = \pi R K_\Sigma \left(\delta^2 - \frac{2w}{K_\Sigma} \right). \tag{52}$$

Using (41), (44) and (45), we obtain

$$a_c = \left(\frac{8R^2 w}{K_\Sigma} \right)^{1/4}, \qquad a(0) = \left(\frac{32R^2 w}{K_\Sigma} \right)^{1/4}, \tag{53}$$

$$P_c = -P(a_c) = 2\pi R w \quad \text{and} \quad \delta_s = \delta[a(0)] = \sqrt{\frac{2w}{K_\Sigma}}. \tag{54}$$

The force-displacement relation in the contact problem without adhesion is a parabola given by

$$P_0 = \pi R K_\Sigma \delta^2 \tag{55}$$

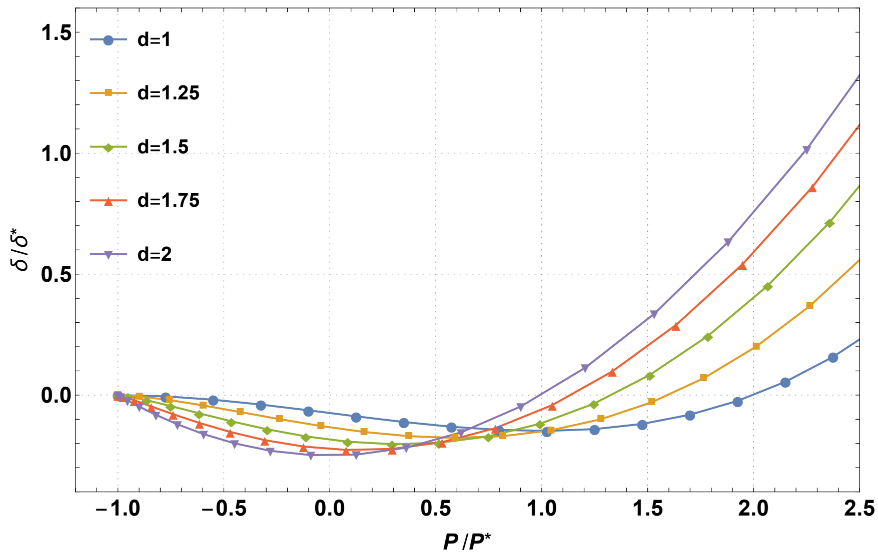

Figure 3: The dimensionless graphs of the force-displacement curves (47) for blunt indenters when the power-law exponent d varies from $d = 1$ (cone) to $d = 2$ (sphere).

corresponding to the case of Winkler foundation, while in the adhesive contact problem, the relation is described by (52), i.e. it is the same parabola shifted by the value P_c in the negative direction of P-axis. Let us present, here, also the $P - \delta$ relation for Hertzian contact given by the formula

$$P = \frac{2^{3/2} E_1}{3\sqrt{B_2}} \delta^{3/2}. \tag{56}$$

The contact pressure can be represented as

$$p\left(r\right) = K_\Sigma \left(\delta - \frac{r^2}{2R}\right) = \frac{K_\Sigma}{2R}\left(a^2 - r^2\right) - \sqrt{2K_\Sigma w}. \tag{57}$$

Zero contact pressure is achieved at the radius r_0

$$r_0 = \sqrt{a^2 - 2R\sqrt{\frac{2w}{K_\Sigma}}}. \tag{58}$$

Maximum contact pressure is at $r = 0$

$$p_{max} = \frac{K_\Sigma a^2}{2R} - \sqrt{2K_\Sigma w}. \tag{59}$$

Substituting $d = 2$ into (47), we obtain the following dimensionless equation

$$\frac{P}{P_c} = \left(\frac{a}{a_c}\right)^4 - 2\left(\frac{a}{a_c}\right)^2, \tag{60}$$

In the same way equations (47) and (48) can be transformed in the following dimensionless equations

$$\frac{\delta}{\delta_s} = \left(\frac{a}{a_c}\right)^2 - 1. \tag{61}$$

and

$$\frac{P}{P_c} = \left(\frac{\delta}{\delta_s}\right)^2 - 1. \tag{62}$$

5.2. Conical indenters

For a conical indenter of semi-vertical angle $\pi/2-\alpha$, $d=1$, $f(r)=B_1 r$, and $B_1=\tan\alpha$. For a linearized treatment to be possible, α must be small compared with 1 and $\tan\alpha = B_1 \approx \alpha$.

It follows from (41) and (42) that

$$\begin{aligned} P &= \pi K_\Sigma \left(\frac{1}{3}B_1 a^3 - \sqrt{\frac{2w}{K_\Sigma}}a^2\right) \\ \delta &= B_1 a - \sqrt{\frac{2w}{K_\Sigma}}. \end{aligned} \tag{63}$$

and from (49) one can get the explicit force-displacement relation

$$P = \frac{\pi K_\Sigma}{3}\left[\frac{1}{B_1}\left(\delta + \sqrt{\frac{2w}{K_\Sigma}}\right)\right]^2\left(\delta - 2\sqrt{\frac{2w}{K_\Sigma}}\right). \tag{64}$$

Similar to the case of a spherical indenter, in the case of non-adhesive contact corresponding to a Winkler foundation, equation (64) takes the simple form

$$P = \frac{\pi K_\Sigma \delta^3}{3B_1^2}. \tag{65}$$

The Hertz solution (56) in the case of a conical indenter takes the form

$$P = \frac{2E_1}{\pi B_1(1-\nu_1^2)}\delta^2. \tag{66}$$

The contact radius at $P=0$ and the shift of the origin of the displacement axis δ_s are, respectively,

$$a(0) = \frac{3}{B_1}\sqrt{\frac{2w}{K_\Sigma}}, \qquad \delta_s = 2\sqrt{\frac{2w}{K_\Sigma}}. \tag{67}$$

It is known that both the Vickers and Berkovich indenters have the same projected area (A) to depth (δ) $A \approx 24.5\delta^2$, see, for example, [34]. Hence, one can consider an equivalent cone $\delta = B_1 a$ such that

$$A(\delta) = 24.5\delta^2 = \pi(\delta/B_1)^2.$$

Hence, the shape constant of the equivalent cone is $B_1 = \sqrt{\pi/24.5} = 0.358$. The apex semi-angle γ of the equivalent cone is $\gamma \cong 70.3^o$. If this cone indents a Winkler-Fuss layer then the asymptotic parameter

$$\varepsilon = \cot\gamma = B_1 = 0.358 < 1,$$

This means that we can apply our asymptotic approach.

5.3. Examples of specific materials

Let us consider, as a first example, the diamond-like carbon (DLC) films prepared by the Plasma Enhanced Chemical Vapour Deposition (PECVD). Park and Kwon, [39], measured that $w = 17.85 \pm 0.06$ N/m for such films.

Let us assume that the films are connected to rigid substrate through an interlayer of plasma sprayed tungsten-carbide (WC). The elastic moduli and Poisson's ratios of DLC and WC are respectively

$$E_{DLC} = 100 \text{ GPa}, \quad \nu_{DLC} = 0.2, \quad E_{WC} = 600 \text{ GPa}, \quad \nu_{WC} = 0.31. \tag{68}$$

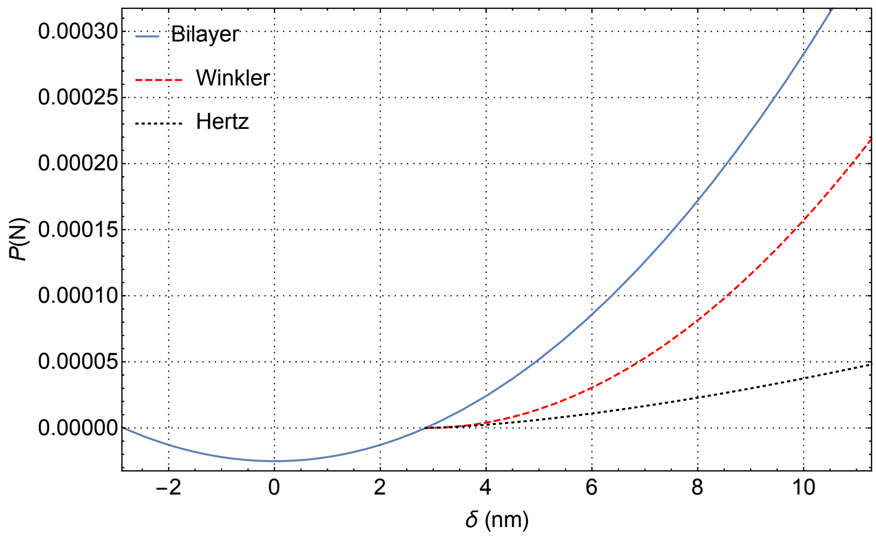

Figure 4: The dimensional $P - \delta$ curve for Example 1 in case of spherical indenters with the physical parameters given by equation (68). The solid line is the $P - \delta$ curve for adhesive bilayer solution (52); the dashed line is the same curve for non-adhesive solution (55); and the dotted line is the same line in the Hertz solution (56) for an elastic half-space made of the material of the layer.

Hence, it follows from (30) that $K_\Sigma = 4.9 \times 10^{-9}$ N/m^3. For our numerical simulations, we will accept that the work of adhesion between the indenter and the DLC layer is $w = 20$ N/m, $h_l = h_g = 20$ nm. According to [40], [41] radii of Berkovich indenters may vary from 40 nm for super sharp indenters to 250 nm for indenters after several months of continuous use. A blunt tip after a year may have 400 nm radius [11]. Let us assume that $R = 200$ nm. Then at penetration of 10 nm, the contact radius of non-adhesive contact with a Winkler-Fuss foundation would be about 63 nm.

Figures 4 and 5 display the force-displacement curves for spherical (52) and equivalent conical (64) indenters. These curves are compared with non-adhesive Hertz solution for an elastic half-space having material properties of the film and with non-adhesive contact with a Winkler-Fuss elastic foundation having $K_\Sigma = 4.9 \times 10^{-9}$ N/m^3 calculated for the coating and the interlayer. The origin of coordinates for these non-adhesive solutions are shifted by the corresponding δ_s. One can see that, the contact force required for the displacement of the indenter in the bilayer system exceeds, both the Winkler foundation and the classical Hertz which is clearly due to the effect of the work of adhesion. Thus, ignoring the effect of the adhesion will result in considerable errors.

As the second example, we consider hard ceramic $\alpha - \mathrm{Al_2O_3}$ (Aluminium Oxide) coating bounded to the substrate through $\mathrm{Ti} - 6\mathrm{Al} - 4\mathrm{V1}$ (Alpha Beta Titanium Alloy). The elastic moduli and Poisson ratios of $\alpha - \mathrm{Al_2O_3}$ and $\mathrm{Ti} - 6\mathrm{Al} - 4\mathrm{V1}$ are, respectively,

$$E_{\mathrm{Al_2O_3}} = 300 \text{ GPa}, \quad \nu_{\mathrm{Al_2O_3}} = 0.21, \qquad E_{\mathrm{Ti-6Al-4V}} = 110 \text{ GPa}, \quad \nu_{\mathrm{Ti-6Al-4V}} = 0.31. \tag{69}$$

The value of K_Σ follows, again, from (30) and is calculated as $K_\Sigma = 5.252 \times 10^{-9}$ N/m^3. The illustration of numerical calculations are performed assuming that the work of adhesion between the indenter and aluminium oxide is $w = 20$ N/m.

In Figures 6 and 7 the force-displacement curves for spherical (52) and equivalent conical (64) indenters are illustrated. Once again, these curves are compared with non-adhesive Hertz solution and with non-adhesive contact with a Winkler-Fuss elastic foundation which, now, has the stiffness $K_\Sigma = 5.252 \times 10^{-9}$ N/m^3 calculated for the coating and the interlayer. The origin of coordinates

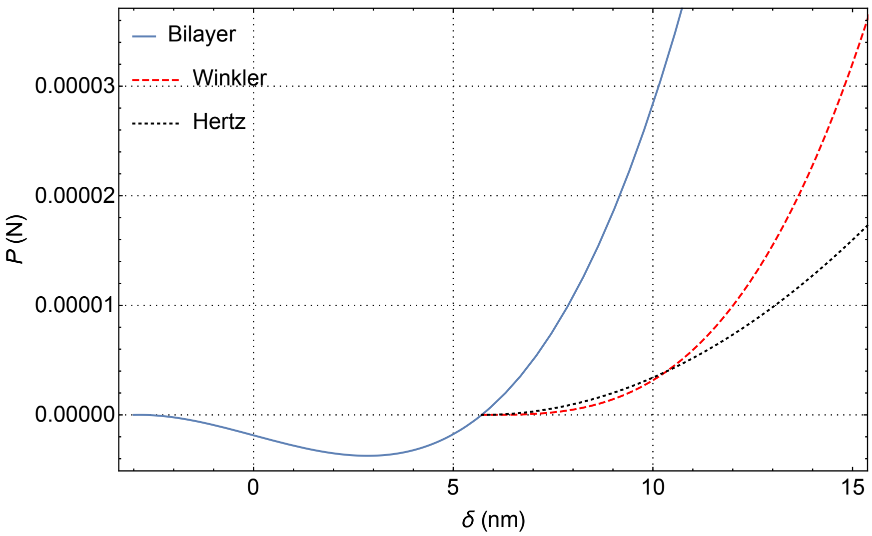

Figure 5: The dimensional $P - \delta$ curve for Example 1 in case of conical indenters with the physical parameters given by equation (68). The solid line is the $P - \delta$ curve for adhesive bilayer solution (64); the dashed line is the same curve for non-adhesive solution (65); and the dotted line is the same line in the Hertz solution (66) for an elastic half-space made of the material of the layer.

for these non-adhesive solutions are shifted by the corresponding δ_s. As before, in both figures, we clearly observe that for the same distance of approach, the bilayer system requires a greater contact force than the Winkler-Fuss and Hertz model implying that, at the nanoscale, the effect of adhesion should be taken into account to avoid significant errors.

Conclusions

Problems of contact between a rigid convex indenter and an elastic thin compressible layer bonded to rigid substrate were studied in a number of publications. We have reviewed and examined various approaches to the problems. It has been shown that many approximate solutions are in essence the solution to the problem of contact between the indenter and a Winkler-Fuss elastic foundation. On the other hand, asymptotic approaches to the problems provide mathematical justification to the use of the Winkler-Fuss elastic foundation. However, most of the asymptotic approaches are rather sophisticated. Only relatively recently simple asymptotic approaches have been developed and applied to the contact problems. Assuming that the thickness of the layer is much less than characteristic dimension of the contact area, it has been shown that the GKN (Goldenveizer-Kaplunov-Nolde) method [26] that was originally developed for applications in the theory of plates and shells, may be applied directly to variables of the contact problem formulation. It is easy to follow the method and naturally it has been shown that the 0-th asymptotic approximation of the problem for a thin layer, isotropic or transversely isotropic, is actually the problem for a layer of springs (the Winkler-Fuss elastic foundation). The GKN approach has been compared with another simple asymptotic approach, the AM (Argatov-Mishuris) one [19]. We argue that although the GKN and AM approaches are mathematically equivalent, the GKN approach has several advantages in producing series, formulating the boundary conditions and writing expressions for displacements and stresses acting in the elastic layer.

The axisymmetric adhesive contact has been studied in the framework of the JKR theory for the leading-order asymptotic approximation of the bi-layer system (the film and the glue layer). The JKR approach has been generalized to the case of the punch shape being described by an arbitrary

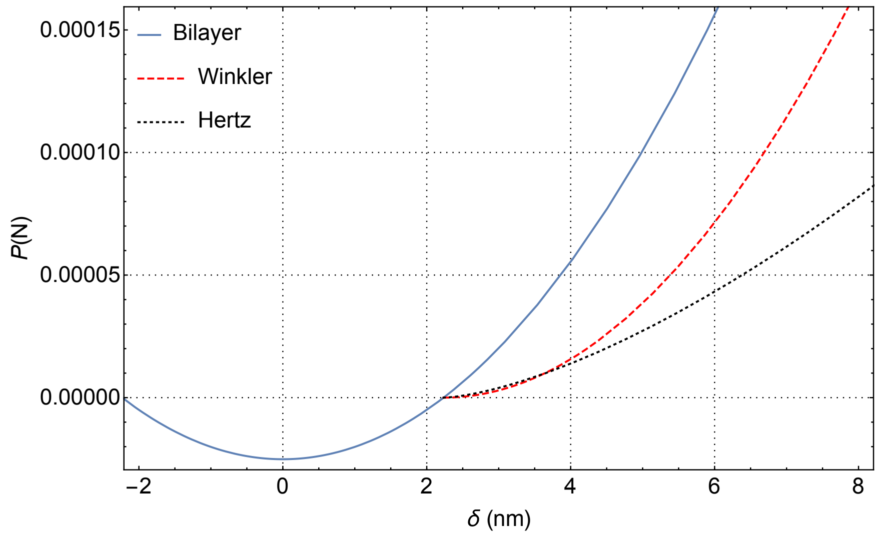

Figure 6: The dimensional $P - \delta$ curve for Example 2 in case of spherical indenters with the physical parameters given by equation (69). The solid line is the $P - \delta$ curve for adhesive bilayer solution (52); the dashed line is the same curve for non-adhesive solution (55); and the dotted line is the same line in the Hertz solution (56) for an elastic half-space made of the material of the layer.

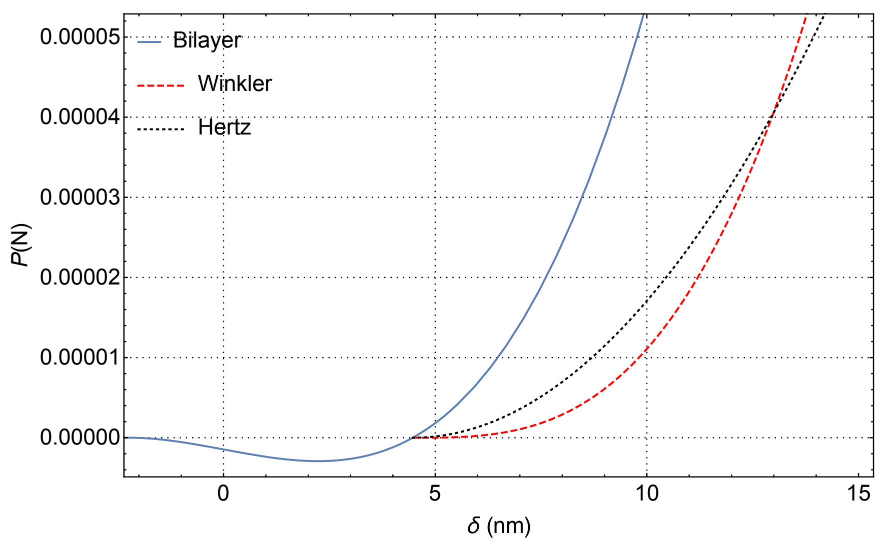

Figure 7: The dimensional $P - \delta$ curve for Example 2 in case of conical indenters with the physical parameters given by equation (69). The solid line is the $P - \delta$ curve for adhesive bilayer solution (64); the dashed line is the same curve for non-adhesive solution (65); and the dotted line is the same line in the Hertz solution (66) for an elastic half-space made of the material of the layer.

blunt axisymmetric indenter. Connections of the results obtained to problems of nanoindentation in the case of the indenter shape near the tip has some deviation from its nominal shape are discussed. The solutions to particular cases of indentation by a spherical indenter and an equivalent conical one have also been discussed in detail for two materials glued to a rigid substrate. It is argued that solutions to the indentation problems should take into account not only the elastic properties of the interlayer but also the effects of adhesion.

Acknowledgements

The work was initiated as a part of activities of the CARBTRIB International Network supported by the Leverhulme Trust. The authors are grateful to the Leverhulme Trust for the support of their collaboration.

BE and FB are grateful to TÜBİTAK via the 2221 - Fellowships for Visiting Scientists and Scientists on Sabbatical Leave for the financial support during the stay of FB at Anadolu University. BE also acknowledges the Scientific Projects of Anadolu University (grant number 1508F603).

References

[1] J.C. Sánchez-López, A. Fernández, Doping and alloying effects on DLC coatings, in: Tribology of diamond-like carbon films, Springer, (2008), pp. 311–338.

[2] K. Taube, M. Grischke, K. Bewilogua, Improvement of carbon-based coatings for use in the cold forming of non-ferrous metals, Surf. Coat. Technol. 68 (1994) 662–668.

[3] J.S. Wang, Y. Sugimura, A.G. Evans, W.K. Tredway, The mechanical performance of DLC films on steel substrates, Thin Solid Films 325 (1-2) (1998) 163–174.

[4] T. Michler, M. Grischke, K. Bewilogua, A.Hieke, Continuously deposited duplex coatings consisting of plasma nitriding and ac: H: Si deposition1, Surf. Coat. Technol. 111 (1) (1999) 41–45.

[5] G.N. Kalei, Some results of microhardness test using the depth of impression, Mashinovedenie 4 (3) (1968) 105–107.

[6] B.A. Galanov, O.N. Grigor'ev, Y.V. Mil'man, I.P. Ragozin, Determination of the hardness and Young's modulus from the depth of penetration of a pyramidal indentor. Strength of Materials, 15, (1983) 1624–1628.

[7] D. Carnelli, R. Lucchini, M. Ponzoni, R. Contro, and P. Vena, Nanoindentation testing and finite element simulations of cortical bone allowing for anisotropic elastic and inelastic mechanical response. J. Biomech. 44(10), (2011) 1852.

[8] E.L. Kossovich, F.M. Borodich, S.A. Epshtein, B.A. Galanov, M.G. Minin, V.A. Prosina, Mechanical, structural and scaling properties of coals: Depth-sensing indentation studies. Appl. Phys. A 125: 195 (2019).

[9] Y. Xia, P. Duan. J. Chen, Modelling the nanomechanical responses of biofilms grown on the indenter probe. Processes 6: 84 (2018).

[10] I. I. Argatov, F. M. Borodich, S. A. Epshtein, and E. L. Kossovich, Contact stiffness depth-sensing indentation: Understanding of material properties of thin films attached to substrates. Mech. Mater. 114 (2017) 172–179.

[11] S.J. Bull, Nanoindentation of coatings, J. Phys. D: Appl. Phys. 38 (24) (2005): R393-R413.

[12] P. Duana, R.Toumpaniari, S. Partridge, M.A. Birch, P.G. Genever, S.J.Bull, K.W. Dalgarno, A.W. McCaskie, J. Chen, How cell culture conditions affect the microstructure and nanomechanical properties of extracellular matrix formed by immortalized human mesenchymal stem cells: An experimental and modelling study. Materials Science and Engineering: C 89 (2018) 149–159.

[13] F.M. Borodich, S.J. Bull, S.A. Epshtein, Nanoindentation in studying mechanical properties of heterogeneous materials, J. Min. Sci. 51 (3) (2015) 470–476.

[14] S.A. Epshtein, F.M. Borodich, S.J. Bull, Evaluation of elastic modulus and hardness of highly inhomogeneous materials by nanoindentation, Appl. Phys. A 119 (1) (2015) 325–335.

[15] S.I. Bulychev, V.P. Alekhin, M.K.Shorshorov, A.P. Ternovskij, G.D. Shnyrev, Determination of Young modulus by the hardness indentation diagram, Zavodskaya Laboratoriya 41 (9) (1975) 1137–1140.

[16] J. Menčík, D. Munz, E. Quandt, E.R. Weppelmann, M.V. Swain, Determination of elastic modulus of thin layers using nanoindentation, J. Mater. Res. 12 (9) (1997) 2475–2484.

[17] E.L. Kossovich, F.M. Borodich, S.J. Bull, S.A. Epshtein, Substrate effects and evaluation of elastic moduli of components of inhomogeneous films by nanoindentation, Thin Solid Films 619 (2016) 112–119.

[18] L.A. Aghalovyan, Asymptotic theory of anisotropic plates and shells, World Scientific Singapore, 2015.

[19] I. Argatov, G. Mishuris, Contact mechanics of articular cartilage layers: Asymptotic models, Vol. 50, Springer, 2015.

[20] F.M. Borodich, B.A. Galanov, N.V. Perepelkin, D.A. Prikazchikov, Adhesive contact problems for a thin elastic layer: Asymptotic analysis and the JKR theory, Math. Mech. Solids (2018) DOI:10.1177/1081286518797378.

[21] V.M. Aleksandrov, S.M. Mkhitaryan, Contact problems for bodies with thin coatings and interlayers, Nauka, Moskow, 1983.

[22] V.M. Aleksandrov, Some contact problems for the elastic layer, J. Appl. Math. Mech. 27 (4) (1963) 1164–1174.

[23] V.M. Aleksandrov, I.I. Vorovich, Contact problems for the elastic layer of small thickness, J. Appl. Math. Mech. 28 (2) (1964) 425–427.

[24] K.L. Johnson, Contact Mechanics, Cambridge University Press, Cambridge, 1985.

[25] A.L. Goldenveizer, Derivation of an approximate theory of bending of a plate by the method of asymptotic integration of the equations of the theory of elasticity, J. Appl. Math. Mech. 26(4) (1962) pp. 1000-1025.

[26] A.L. Goldenveizer, J.D. Kaplunov, E.V. Nolde, On Timoshenko-Reissner type theories of plates and shells, Int. J. Solids Struct. 30 (5) (1993) 675–694.

[27] B. Erbaş, E. Yusufoğlu, J. Kaplunov, A plane contact problem for an elastic orthotropic strip, J. Eng. Math. 70 (4) (2011) 399–409.

[28] J. Kaplunov, D. Prikazchikov, L. Sultanova, Justification and refinement of Winkler-Fuss hypothesis, Z. Angew. Math. Phys. 69(3) (2018) 80.

[29] K. Kendall, Molecular adhesion and its applications: the sticky universe, Springer Science & Business Media, 2001.

[30] K.L. Johnson, K. Kendall, A.D. Roberts, Surface energy and the contact of elastic solids, in:Proc. R. Soc. London, Ser. A: Math. Phys. Eng. Sci. Vol. 324 (1971) pp.301–313.

[31] F.M. Borodich, L.M. Keer, Contact problems and depth-sensing nanoindentation for frictionless and frictional boundary conditions, Int. J. Solids Struct. 41 (9) (2004) 2479–2499.

[32] F.M. Borodich, L.M. Keer, C.S. Korach, Analytical study of fundamental nanoindentation test relations for indenters of non-ideal shapes, Nanotechnology 14 (7) (2003) 803.

[33] F.M. Borodich, B.A. Galanov, M.M. Suarez-Alvarez, The JKR-type adhesive contact problems for power-law shaped axisymmetric punches, J. Mech. Phys. Solid 68 (2014) 14–32.

[34] F.M. Borodich, The Hertz-type and adhesive contact problems for depth-sensing indentation, in: Adv. Appl. Mech. Vol. 47, Elsevier, (2014), pp. 225–366.

[35] K.L. Johnson, K. Kendall, A.D. Roberts, Surface energy and the contact of elastic solids, Proc. R. Soc. London, Ser. A: Math. Phys. Eng. Sci. 324(1558) (1971) pp.301-313.

[36] B.V. Derjaguin, Untersuchungen über die Reibung und Adhäsion, IV. Colloid. Polym. Sci. 69(2) (1934) pp.155-164.

[37] F.M. Borodich, B.A. Galanov, L.M. Keer, M.M. Suarez-Alvarez, The JKR-type adhesive contact problems for transversely isotropic elastic solids, Mech. Mater. 75 (2014) 34-44.

[38] F.M. Borodich, B.A. Galanov, Contact probing of stretched membranes and adhesive interactions: graphene and other two-dimensional materials, Proc. R. Soc. London, Ser. A: Math. Phys. Eng. Sci. 472(2195) (2016) 20160550.

[39] H.S. Park, D. Kwon, An energy approach to quantification of adhesion strength from critical loads in scratch tests, Thin Solid Films 307(1-2) (1997) pp.156-162.

[40] S.J. Bull, Analysis methods and size effects in the indentation fracture toughness assessment of very thin oxide coatings on glass, C.R. Mec. 339(7-8) (2011) 518-531.

[41] J. Chen, S.J. Bull, Modelling the limits of coating toughness in brittle coated systems, Thin Solid Films 517(9) (2009) 2945-2952.

[42] F.M. Borodich, B.A. Galanov, S.N. Gorb, Y.I. Prostov, Adhesive contact problems at macro and nano scales, Vol. 1, Österreichische Tribologische Gesellschaft, 2011.

[43] F. Yang, Asymptotic solution to axisymmetric indentation of a compressible elastic thin film, Thin Solid Films 515 (4) (2006) 2274–2283.